Long-Period Fiber Gratings for Mode Coupling in Mode-Division-Multiplexing Systems

Daulet Askarov and Joseph M. Kahn, *Fellow, IEEE*

***Abstract*—In mode-division-multiplexing systems, multi-input multi-output (MIMO) equalization is used to compensate for linear impairments, including modal dispersion (MD) and modal crosstalk. The MIMO equalizer memory length depends on the group delay (GD) spread arising from MD. The GD spread arising from MD can be significantly reduced by introducing strong mode coupling via mode scramblers. We study the design of such mode scramblers implemented as long-period multimode fiber gratings for systems using $D = 12$ modes (six spatial modes). By optimizing the grating chirp function, we minimize the mode-dependent loss (MDL) of the grating while ensuring full intergroup mode coupling. We find a design yielding MDL and mode-averaged loss in the C band not exceeding 0.36 and 0.45 dB, respectively. We also verify the effect of such mode scramblers on the GD scaling of a long-haul system, demonstrating that the scramblers reduce the scaling of GD spread with length from a linear to a square-root dependence, as expected in the strong coupling regime.**

***Index Terms*—Fiber gratings, mode coupling, multiplexing, optical fibers.**

I. Introduction

As Internet traffic continues growing rapidly, the capacity of long-haul single-mode fiber (SMF) transmission systems is approaching information-theoretic limits [1]. Parallel transmission in multi-core fibers or mode-division multiplexing (MDM) in multi-mode fibers (MMFs) have been proposed as methods to increase per-fiber capacity [2]–[4]. Transmission capacity in MDM systems ideally scales in proportion to the number of modes employed [3], [4]. MMF is currently widely used for short-range optical links because of relaxed connector alignment tolerances and reduced transceiver component costs [5].

Current long-haul SMF systems already employ multiplexing in the two polarization modes, and use coherent detection and digital signal processing (DSP) to compensate for chromatic dispersion (CD), polarization-mode dispersion (PMD) and polarization crosstalk [6], [7]. A 2×2 MIMO equalizer is used to compensate for the PMD and crosstalk. Similarly, in an MDM system employing D modes (including spatial and polarization degrees of freedom), a $D \times D$ MIMO equalizer is used to compensate for modal dispersion (MD) and crosstalk. The computational complexity of this MIMO equalizer increases with the number of modes D because of an increased dimensionality, and because of the group delay (GD) spread associated with MD, which can far exceed the GD spread associated with PMD or CD. One of the primary goals of MDM is reducing energy consumption per transmitted bit [8]. Hence, reducing GD spread and the computational complexity and resulting energy consumption of the MIMO equalizer are particularly important for the feasibility of MDM systems.

One way of reducing the GD spread in MMF is by inducing strong mode coupling in the fiber [9], [10]. This approach is synergistic with a low uncoupled GD spread, which tends to facilitate mode coupling. In the presence of mode coupling, by generalizing the concept of the polarization correlation length in SMF [11], [12] one can define a modal correlation length over which modal fields [13] in a MMF are correlated. In the strongly coupled MDM system, when the total system length is much longer than the correlation length, the GD spread due to MD is reduced substantially, and scales in proportion to the square-root of the total system length [9], [10].

In addition to reducing GD spread and the related MIMO equalization complexity, strong mode coupling also mitigates the effects of mode-dependent loss or gain (collectively referred to as MDL), thus increasing average channel capacity and reducing outage probability [3], [14]. Strong mode coupling and MD create frequency diversity, which further reduces the outage probability [15].

Unintentional mode coupling can arise from random index perturbations, bends, twists or crosstalk at modal (de)multiplexers and other components. Such unintentional mode coupling easily occurs between modes within the same mode group, an effect known as intragroup mode coupling, due to close values of modal propagation constants with subsequent strong longitudinal spatial correlation. However, coupling between modes from different mode groups, known as intergroup mode coupling, is harder to achieve, and might require inserting mode scramblers in each fiber span. One way of implementing such a scrambler is to use a long-period multimode fiber grating (LPMFG) with grating period tuned to phase-match modes from adjacent mode groups. However, a careful design is required to ensure full intergroup coupling and minimal coupling to leaky unguided modes. Such gratings are typically fabricated using illumination of the germanosilicate fiber core material with ultraviolet laser light, which induces a permanent modification of the refractive index [16].

In this paper, we study LPMFGs for mode coupling in MDM systems supporting $D = 12$ modes. Assuming a graded- index with graded depressed cladding (GIGDC) profile, which achieves low uncoupled GD spread [17], we calculate the guided

Manuscript received March 12, 2015; revised June 1, 2015 and July 14, 2015; accepted July 15, 2015. Date of publication July 20, 2015; date of current version August 17, 2015. This work was supported by in part by the National Science Foundation under Grant ECCS-1101905, a Google Research Award, and Corning, Inc.

The authors are with the E. L. Ginzton Laboratory, Department of Electrical Engineering, Stanford University, Stanford, CA 94305, USA (e-mail: daskarov@stanford.edu; jmk@ee.stanford.edu).

Color versions of one or more of the figures in this paper are available online at http://ieeexplore.ieee.org.

Digital Object Identifier 10.1109/JLT.2015.2459070

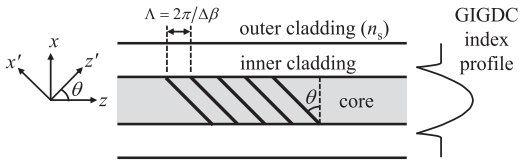

Fig. 1. Diagram of a tilted fiber grating. Λ: grating period, θ: grating tilt.

and leaky modal field profiles, propagation constants and uncoupled GDs. We then model propagation of both guided and leaky modes in the LPMFG by using coupled mode theory [18]. By using a multi-section LPMFG with each section having a slightly different effective grating period, we optimize for minimal coupling to the leaky modes while maintaining full intergroup mode coupling. We show that inserting an LPMFG in each fiber span indeed reduces the scaling of GD spread with distance from a linear to a square-root dependence, as expected for strong mode coupling.

The remainder of the paper is organized as follows. Section II describes modeling of modal propagation in LPMFGs and the design methodology for LPMFGs. Section III presents numerical results for our design of a single LPMFG and discusses its application in MDM systems. Sections IV and V provide discussion and conclusion, respectively.

II. Design and Modeling Methodology

The diagram of a tilted fiber grating is shown in Fig. 1. We assume that LPMFG has the same GIGDC refractive index profile as the transmission fiber and supports *D* guided modes.

A. Guided and Leaky Modes

In principle, any electric field distribution launched into the fiber can be fully decomposed into a set of modes, which may be classified as guided modes or radiation modes.

Guided modes are mutually orthogonal solutions of the wave equation for a given refractive index profile of the fiber. These modes are discrete, and there is a finite number of them supported by a fiber. Because the core, on average, has a higher refractive index than the cladding, a fiber supports at least a pair of degenerate modes, as in SMF, or multiple spatial and polarization modes, as in MMF. In our modeling, guided modes have purely real propagation constants with no leakage, although in practice they get slowly attenuated as a result of material absorption and coupling to radiation modes due to fiber bends and twists.

Radiation modes comprise a continuum of modes whose wavevectors have a component orthogonal to the fiber axis, leading to power leakage. They are also sometimes called cladding modes or unbound modes. Radiation modes are present regardless of the relationship between the refractive indices of the cladding and the medium surrounding it. It is known [19], [20] that the continuum of radiation modes can be conveniently modeled as a discrete set of so-called leaky modes. Leaky modes have complex propagation constants. The imaginary component of the propagation constant of a leaky mode represents the leakage per unit length.

It is known [21] that when the medium surrounding the cladding has a refractive index lower than the cladding, the fiber also supports guided cladding modes. However, this case is of limited practical interest, since deployed fibers are typically coated by a protective polymer coating that has a refractive index higher than the cladding.

In order to properly model modal coupling induced by an LPMFG, we first solve for the guided and leaky modes supported by the LPMFG. We use a numerical vector mode solver based on radial discretization [22] without assuming weak guidance, and including fiber material dispersion. In order to calculate the leaky modes, which in turn approximate a continuum of radiation modes, the solver uses an outer perfectly matched layer terminated with zero boundary condition. We solve for field patterns $\mathbf{E}_{\mathrm{m}}(r,\phi)$ and propagation constants β_m of both leaky and guided modes in a unified manner for modeling coupling in the LPMFG. We also calculate uncoupled GDs per unit length of the guided modes by estimating first derivatives of their propagation constants with respect to optical frequency for later MDM system simulations.

It is known that guided modes in GIGDC fibers form mode groups having nearly equally spaced average propagation constants. The propagation constant spacing $\Delta\beta$ between adjacent mode groups determines the grating period Λ (Fig. 1) required to phase-match those mode groups:

$$\Lambda = \frac{2\pi}{\Delta\beta}. \tag{1}$$

B. Coupled-Mode Propagation

In order to compute the overall coupling matrix describing the LPMFG, we use coupled-mode theory and model propagation of guided and leaky modes in the device for different launching conditions. The evolution of the complex amplitude $a_m(z)$ of the *m*th mode is described by

$$\frac{da_m}{dz} + j\beta_m a_m = -j\sum_n \kappa_{mn} a_n \tag{2}$$

where κ_{mn} is a coupling coefficient between the *m*th and *n*th modes, which in turn can be expressed in terms of an overlap of their normalized mode profiles [18]

$$\kappa_{mn} \approx \frac{\varepsilon_0 \omega}{2\langle \boldsymbol{E}_{tm}, \boldsymbol{H}_{tm}\rangle} \iint \bar{n}(r)\Delta n(z')\boldsymbol{E}_m \cdot \boldsymbol{E}_n dS \tag{3}$$

where

$$\langle \boldsymbol{E}_{tm}, \boldsymbol{H}_{tm}\rangle = \frac{1}{2}\iint (\boldsymbol{E}_{tm} \times \boldsymbol{H}_{tm}) \cdot \hat{z} dS. \tag{4}$$

Here, $\boldsymbol{E}_{tm}$ and $\boldsymbol{H}_{tm}$ are the transverse components of the electric and magnetic field profiles of the *m*th mode, $\bar{n}(r)$is the refractive index profile in the absence of grating index perturbation, and $\Delta n(z')$ is the index perturbation written in the grating along the tilt axis z', as shown in Fig. 1.

In order to compute the integral in Eq. (4), we express the modal electric field distributions in cylindrical coordinates (r,ϕ,z). The exact form depends on the polarization of the modes. The electric field distributions of *p*-polarized modes in polar

coordinates are [18]

$$\boldsymbol{E}_m\left(r,\phi\right) = \begin{bmatrix} E_{rm}\left(r\right)\cos\left(\mu\phi\right) \\ E_{\phi m}\left(r\right)\sin\left(\mu\phi\right) \\ E_{zm}\left(r\right)\cos\left(\mu\phi\right) \end{bmatrix},$$

$$\boldsymbol{E}_n\left(r,\phi\right) = \begin{bmatrix} E_{rn}\left(r\right)\cos\left(\nu\phi\right) \\ E_{\phi n}\left(r\right)\sin\left(\nu\phi\right) \\ E_{zn}\left(r\right)\cos\left(\nu\phi\right) \end{bmatrix}. \quad (5)$$

Here, μ and ν are the azimuthal numbers of the modes numbered *m* and *n* respectively; $E_{rm}(r)$, $E\phi_m(r)$, $E_{zm}(r)$ and $E_{rn}(r)$, $E_{\phi n}(r)$, $E_{zn}(r)$ are the radial, azimuthal and z components of the radial-dependent part of the electric field distributions of modes *m* and *n* respectively.

Similarly, the *m*th and *n*th *s*-polarized modes are [18]

$$\boldsymbol{E}_m\left(r,\phi\right) = \begin{bmatrix} E_{rm}\left(r\right)\sin\left(\mu\phi\right) \\ -E_{\phi m}\left(r\right)\cos\left(\mu\phi\right) \\ E_{zm}\left(r\right)\sin\left(\mu\phi\right) \end{bmatrix},$$

$$\boldsymbol{E}_n\left(r,\phi\right) = \begin{bmatrix} E_{rn}\left(r\right)\sin\left(\nu\phi\right) \\ -E_{\phi n}\left(r\right)\cos\left(\nu\phi\right) \\ E_{zn}\left(r\right)\sin\left(\nu\phi\right) \end{bmatrix}. \quad (6)$$

Before we substitute Eq. (5) or Eq. (6) into (3), we assume that the index modulation of the grating is sinusoidal and is present only in the fiber core region:

$$\begin{aligned}\Delta n\left(z'\right) &= 2\hat{\chi}\left(z'\right)\cos\left(\frac{2\pi}{\Lambda\cos\theta}z' + \hat{\varphi}\left(z'\right)\right) \\ &\approx 2\chi\left(z\right)\cos\left(\frac{2\pi}{\Lambda}\left(z + x\tan\theta\right) + \varphi\left(z\right)\right). \quad (7)\end{aligned}$$

Here, $\hat{\chi}\left(z'\right) \approx \hat{\chi}\left(z\cos\theta\right) = \chi\left(z\right)$ is the modulation depth and $\hat{\varphi}\left(z'\right) \approx \hat{\varphi}\left(z\cos\theta\right) = \varphi\left(z\right)$ is a grating chirp function used to fine tune the local effective grating period. We have assumed that the modulation depth and chirp functions vary slowly, leading to the approximation $z' = z\cos\theta + x\sin\theta \approx z\cos\theta$ in the arguments of these functions. This approximation is applicable because the fiber core diameter is much smaller than the grating length.

We can now compute coupling coefficients between *p*-modes by substituting Eqs. (5) and (7) into (3) and integrating over the azimuthal angle ϕ:

$$\begin{aligned}\kappa_{mn} = &\left\{K_{mn}^{+}\exp\left[+j\left(\frac{2\pi}{\Lambda}z + \varphi\left(z\right)\right)\right]\right. \\ &\left. + K_{mn}^{-}\exp\left[-j\left(\frac{2\pi}{\Lambda}z + \varphi\left(z\right)\right)\right]\right\}\chi\left(z\right) \quad (8)\end{aligned}$$

where

$$\begin{aligned}K_{mn}^{+} = &\frac{\varepsilon_0\omega}{2\left\langle \boldsymbol{E}_{tm}, \boldsymbol{H}_{tm}\right\rangle} \\ &\times\int_0^{r_{co}}\bar{n}(r)r\left[\left(E_{\phi m}E_{\phi n}\right)S\left(r\right)\right. \\ &\left. + \left(E_{rm}E_{rn} + E_{zm}E_{zn}\right)C\left(r\right)\right]dr \quad (9)\end{aligned}$$

$$K_{mn}^{-} = \left(-1\right)^{\mu+\nu}K_{mn}^{+} \quad (10)$$

$$C\left(r\right) = \int_0^{2\pi}\cos\left(\mu\phi\right)\cos\left(\nu\phi\right)\exp\left(j\frac{2\pi}{\Lambda}r\tan\theta\cos\phi\right)d\phi \quad (11)$$

$$S\left(r\right) = \int_0^{2\pi}\sin\left(\mu\phi\right)\sin\left(\nu\phi\right)\exp\left(j\frac{2\pi}{\Lambda}r\tan\theta\cos\phi\right)d\phi. \quad (12)$$

We have grouped together the azimuthal integrations into functions *C*(*r*) and *S*(*r*). To obtain coupling coefficients between *s*–polarized modes, we substitute Eqs. (6) and (7) into Eq. (3) and integrate over ϕ. It can be shown that Eq. (8) still holds for the *s*-modes provided that *C*(*r*) and *S*(*r*) are interchanged in Eq. (9). Note that because of orthogonality, there is no coupling between *p*- and *s*-modes in this model.

One can easily observe from Eqs. (11) and (12) that if the grating is not tilted, i.e. $\theta = 0$, then there is no coupling between modes with different angular symmetries, and in order to induce considerable coupling between those modes, tan θ should be sufficiently large.

By further substituting Eq. (8) into Eq. (2) and using a slowly varying envelope substitution to mathematically isolate coupling effects from propagation:

$$u_m\left(z\right) = a_m\left(z\right)\exp\left(j\bar{\beta}_m z\right) \quad (13)$$

we get the following system of equations

$$\begin{aligned}\frac{du_m}{dz} = &-j\left(\beta_m - \bar{\beta}_m\right)u_m\left(z\right) \\ &-j\sum_{n(n\neq m)}K_{mn}^{+}\chi\left(z\right)u_n\left(z\right) \\ &\times\exp\left(j\left(\bar{\beta}_m - \bar{\beta}_n + \frac{2\pi}{\Lambda}\right)z + j\varphi\left(z\right)\right) \\ &-j\sum_{n(n\neq m)}K_{mn}^{-}\chi\left(z\right)u_n\left(z\right) \\ &\times\exp\left(j\left(\bar{\beta}_m - \bar{\beta}_n - \frac{2\pi}{\Lambda}\right)z - j\varphi\left(z\right)\right). \quad (14)\end{aligned}$$

Here, $\bar{\beta}$ indicates the real part of a propagation constant β.

C. Design Strategy

We note that in the two sums in Eq. (14), only terms corresponding to modes from neighboring mode groups and having the same polarization can have significant coupling to the *m*th mode. The least-confined mode group is also phase-matched to a group of leaky modes, and can potentially couple to them.

We use Eq. (14) to propagate guided and leaky modes in the LPMFG by launching one guided mode at a time, thereby obtaining one column of a $D \times D$ field coupling matrix $\mathbf{M}_c$ describing the LPMFG. From $\mathbf{M}_c$, we can compute mode-averaged and mode-dependent losses of the device [14]:

$$\sigma_{\mathrm{MDL}} = \mathrm{std}\left(\log\left(\mathrm{eig}\left(\boldsymbol{M}_c\cdot\boldsymbol{M}_c^{H}\right)\right)\right) \quad (15)$$

$$\sigma_{\mathrm{MAL}} = \mathrm{mean}\left(\log\left(\mathrm{eig}\left(\boldsymbol{M}_c\cdot\boldsymbol{M}_c^{H}\right)\right)\right). \quad (16)$$

Because for D modes in a graded-index fiber there are a total of $M = \left(\sqrt{4D+1}-1\right)/2$ mode groups [23], to study intergroup coupling effects, the full $D \times D$ matrix $\mathbf{M}_c$ can be reduced to an $M \times M$ mode group power-coupling matrix $\mathbf{P}_c$. Each element of $\mathbf{P}_c$ is formed by averaging squares of magnitudes of the elements from the corresponding block of the field coupling matrix. In order to maintain full intergroup mode coupling, the non-diagonal elements of the matrix $\mathbf{P}_c$ need to be sufficiently large.

We can then optimize the physical parameters of the device, in particular $\varphi(z)$, to minimize losses while maintaining full intergroup mode coupling.

D. LPMFG Scramblers in MDM Systems

After finding a good design for the LPMFG scrambler, we can model use of the scrambler in a long-haul MDM system to investigate the effect on GD spread reduction.

We model field propagation of fiber modes by using a multi-section model [10]. A kth fiber section is modeled as a $D \times D$ matrix $\mathbf{M}^{(k)}$. One can express the overall propagation matrix for a fiber span comprising K sections as

$$\mathbf{M}_t = \prod_{i=0}^{K-1} \mathbf{M}^{(K-i)}. \tag{17}$$

Each of the sections can be expressed as a product of three matrices:

$$\mathbf{M}^{(k)} = \begin{bmatrix} \mathbf{U}_1^{(k)} & 0 & 0 \\ 0 & \mathbf{U}_2^{(k)} & 0 \\ 0 & 0 & \mathbf{U}_3^{(k)} \end{bmatrix} \mathbf{\Lambda}^{(k)} \begin{bmatrix} \mathbf{V}_1^{(k)} & 0 & 0 \\ 0 & \mathbf{V}_2^{(k)} & 0 \\ 0 & 0 & \mathbf{V}_3^{(k)} \end{bmatrix} \tag{18}$$

where the left and right matrices are block-unitary with a number of blocks equal to the number of mode groups M, which describe intragroup coupling in the kth section, and the $\mathbf{\Lambda}^{(k)}$ are frequency-dependent and represent modal dispersion:

$$\mathbf{\Lambda}^{(k)}(\omega) = \begin{bmatrix} e^{-j\omega\tau_1^{(k)}} & 0 & 0 \\ 0 & \ddots & 0 \\ 0 & 0 & e^{-j\omega\tau_D^{(k)}} \end{bmatrix}. \tag{19}$$

Assuming that an LPMFG is placed in each fiber span, we can model the overall propagation matrix for a series of N spans:

$$\mathbf{M} = \prod_{n=0}^{N-1} \mathbf{M}_c \prod_{i=0}^{K-1} \mathbf{M}_{(N-n)}^{(K-i)}. \tag{20}$$

To calculate the end-to-end GD spread of this series of spans with interspersed mode scramblers, we use the GD operator $\mathbf{G}$ [24]:

$$\mathbf{G} = j\frac{d\mathbf{M}}{d\omega}\mathbf{M}^{-1}(\omega). \tag{21}$$

The eigenvectors of $\mathbf{G}$ are principal modes [24], and the eigenvalue of the ith principal mode, τ_i, represents its GD, which we compute numerically. Note that the GD operator definition (21), a generalization of that given in [24], is valid in the presence of MDL. We then calculate the system's end-to-end r.m.s. GD spread as

$$\sigma_{\mathrm{GD}} = \sqrt{\frac{\sum_{i=1}^{D}\left(\tau_i - \langle\tau_i\rangle\right)^2}{D}}. \tag{22}$$

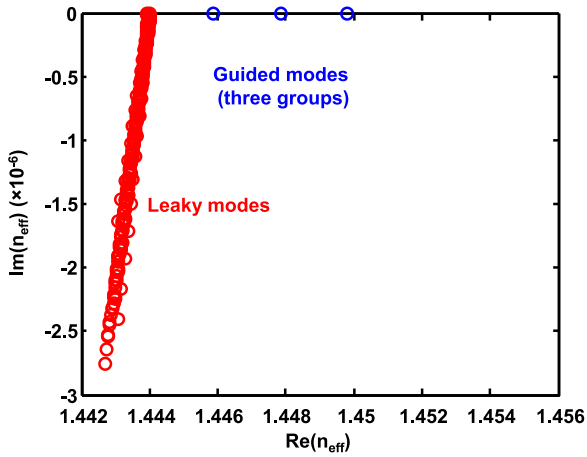

Fig. 2. Propagation constants of leaky and guided modes in GIGDC fiber supporting 12 modes.

III. Results

We fix the numerical aperture of the fiber to be NA $= 0.15$ and the number of guided modes to be $D = 12$, where these modes form $M = 3$ mode groups. For a given NA and D, there is a range of core radii that support the desired number of guided modes D. We choose the core radius such that at the shortest wavelength of the C-band (1530 nm), the next higher-order mode is slightly above cutoff. This optimizes mode confinement and minimizes bending losses.

We use the numerical mode solver described in Section II-A to calculate the electric field profiles of the guided and leaky modes, as well as their propagation constants at a wavelength of 1550 nm (Fig. 2). The solver provides a large number of leaky modes, while only a few of them are critical for calculating the LPMFG coupling matrix. To reduce the computational burden of later simulations, we sort the leaky modes according to magnitudes of their K_{mn}^{+} coefficients relative to the guided modes and consider only the 40 having the largest normalized coupling coefficients.

We calculate the average difference of the propagation constants between adjacent mode groups $\Delta\beta$, which yields a corresponding grating period $\Lambda = 787$ μm. We choose a constant refractive index modulation depth $\chi(z) = 1.5 \times 10^{-4}$ and a large grating tilt angle $\theta = 85$ to achieve sufficient coupling between modes with different angular symmetries.

We further parameterize $\varphi(z)$ as a piecewise-linear function with ten sections, each section having a certain length and slope.

Given these 20 section lengths and slopes, we can calculate the field coupling matrix $\mathbf{M}_c$ and the corresponding r.m.s. MDL, as well as the non-diagonal elements of the mode group power coupling matrix $\mathbf{P}_c$. This sets an optimization problem with 20

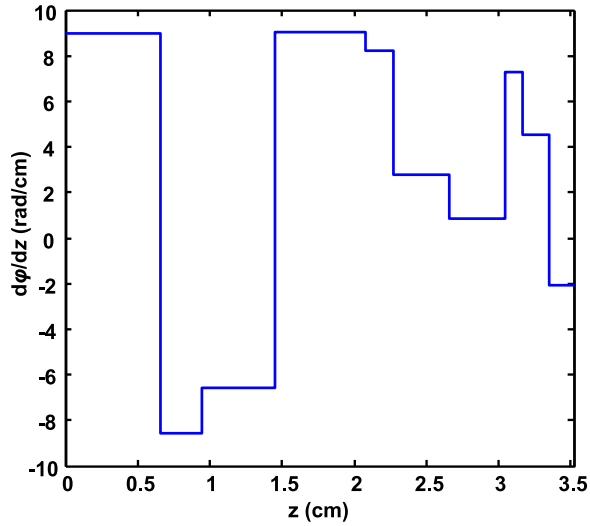

Fig. 3. Longitudinal slope variation of the grating chirp $\varphi(z)$ for the best design found.

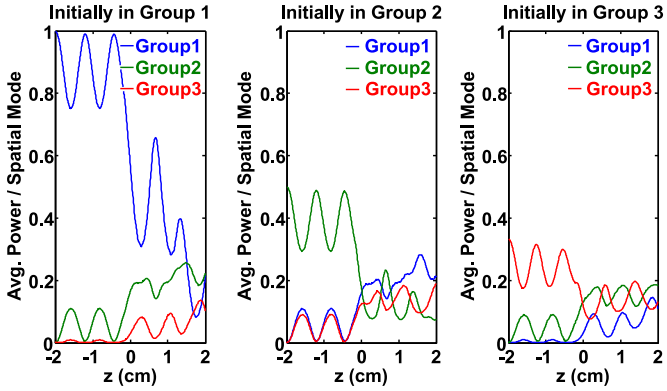

Fig. 4. Evolution of powers in different mode groups in an LPMFG.

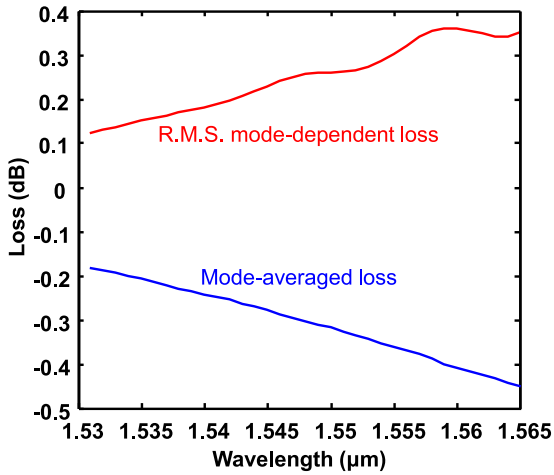

Fig. 5. Mode-averaged and mode-dependent loss of a single LPMFG.

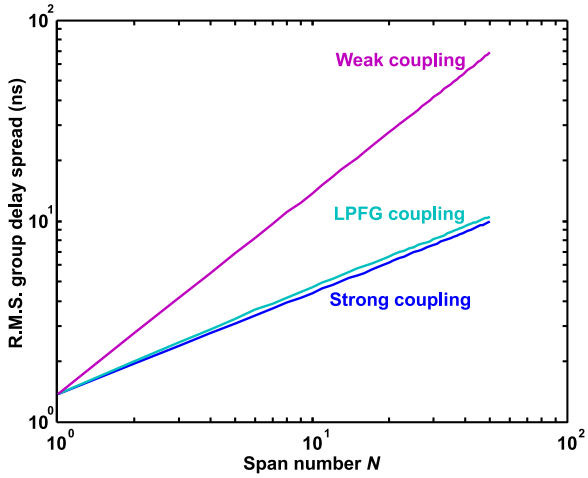

Fig. 6. Group delay spread accumulation in a long-haul MDM system.

variables. The objective function to be minimized is the r.m.s. MDL. We further reduce the search space by only considering designs with non-diagonal elements of the matrix $\mathbf{P}_c$ above a threshold of 0.12. This threshold value was determined to be sufficient for inducing strong overall coupling. The best design $\varphi(z)$ found after multiple runs of genetic algorithm has the section slopes and lengths shown in Fig. 3.

Evolution of the power in different mode groups for different launching conditions for the optimized LPMFG design is shown in Fig. 4. We observe that the optimized design indeed provides significant intergroup coupling.

To verify minimal coupling to unguided leaky modes, we calculate mode-averaged loss and r.m.s. MDL after computing $\mathbf{M}_c(\lambda)$ for the entire C band (Fig. 5). We observe that MDL does not exceed 0.36 dB, and mode-averaged loss is below 0.45 dB.

For numerical simulation of GD spread accumulation in MDM systems, we choose a fiber section length of 1 km and a fiber span length of 100 km. We calculate the r.m.s. GD spread averaged over 300 different system realizations as a function of the span number N. In Fig. 6, we compare the accumulation of r.m.s. GD spread with number of spans N for three cases: (a) only intragroup coupling is present (weak coupling); (b) each span has intragroup coupling and an LPMFG scrambler is inserted between spans; and (c) each span has ideal strong coupling, i.e., a random unitary matrix $\mathbf{U}^{(n)}$ is used in each span instead of $\mathbf{M}_c$ in Eq. (20). We clearly observe that placing an LPMFG scrambler into each span enables strong coupling, causing the r.m.s. GD spread to accumulate in proportion to the square-root of the propagation distance. By changing the operating wavelength, we verify the same GD reduction behavior across the entire C band.

IV. Discussion

Our results demonstrate that a carefully designed LPMFG can be used as a mode scrambler with MDL of at most 0.36 dB and mode-averaged loss of 0.45 dB in the C band. We have shown that placing such a device in every fiber span can induce strong mode coupling in a multi-span system.

A possible alternative mode scrambler implementation would employ a pair of back-to-back photonic lanterns [25]. Ideal

photonic lanterns with adiabatic tapering can theoretically achieve zero MDL. However, such devices might be more sensitive to vibrations and might require more careful handling than LPMFGs.

Traditional mode scramblers, such as devices based on placing a fiber between two corrugated surfaces to induce microbending [26]–[28], are expected to have significantly higher losses than LPMFGs, because tight bending of a fiber facilitates coupling to radiation modes. Another traditional mode scrambler design is based on concatenating several sections of fiber with different index profiles [29], [30]. These mode scramblers are also expected to have higher losses than LPMFGs because of the incomplete overlap between modes in different fiber types, which implies strong coupling to radiation modes. Furthermore, it is not clear how to ensure full mode coupling and low MDL in these traditional mode scrambler designs.

In this study, we limited our LPMFG design strategy to optimizing a piecewise-linear chirp $\varphi(z)$ with ten sections. Given a design strategy with a larger number of sections or allowing variation of other design parameters of the LPMFG, it might be possible to further reduce or possibly even eliminate the MDL of the scrambler.

An alternate method to reduce the MDL in an LPMFG scrambler is to use a refractive index profile that induces a non-uniform spacing of the mode group propagation constants, e.g., a step-index profile. This non-uniform spacing enables more precise control of phase matching between mode groups, facilitating minimization of coupling to leaky modes. Such a fiber would likely have a larger GD spread per unit length than the GIGDC profile, but a short LPMFG would have a very small GD. This approach would require adiabatic index transitions between the LPMFG and the transmission fiber, in order to achieve lossless conversion between their respective eigenmodes without intergroup coupling.

Achieving very low MDL would allow placement of multiple scramblers within each fiber span, further reducing the GD spread without introducing significant MDL.

A potential concern for LPMFG design is sensitivity of the modal propagation constants to the core radius and temperature variations.

The propagation constant spacing between adjacent mode groups is inversely proportional to the fiber core radius, and is thus sensitive to fluctuations in core radius occurring in fabrication. The impact of such core radius errors can be minimized if one first measures the modal propagation constants in a section of fiber and then fabricates the LPMFG with a grating period appropriate for that section of fiber.

Temperature variations cause transverse and longitudinal expansion and contraction of an LPMFG. Calculations show that these thermal effects have a negligible impact on the GD spread reduction obtained by using LPMFGs in a multi-span system.

V. Conclusion

In MDM systems, strong mode coupling can significantly reduce the modal GD spread, thereby reducing signal processing complexity. Likewise, strong mode coupling can reduce MDL and induce frequency diversity, increasing average capacity and reducing outage probability.

Intragroup mode coupling already occurs in typical transmission fibers. LPMFGs can be used as mode scramblers to induce intergroup coupling, thus ensuring strong overall coupling.

We described a design procedure for an LPMFG mode scrambler, presenting results for $D = 12$ modes. The optimized design has a maximum of 0.36 dB MDL and 0.45 dB of mode-averaged loss across the C band. By studying the r.m.s. GD accumulation in a multi-span system, we verified that the LPMFG scrambler induces strong coupling when placed in each span.

References

[1] R.-J. Essiambre, G. Kramer, P. J. Winzer, G. J. Foschini, and B. Goebel, "Capacity limits of optical fiber networks," *J. Lightw. Technol.*, vol. 28, no. 4, pp. 662–701, Feb. 2010.

[2] T. Morioka, Y. Awaji, R. Ryf, P. J. Winzer, D. Richardson, and F. Poletti, "Enhancing optical communications with brand new fibers," *IEEE Commun. Mag.*, vol. 50, no. 2, pp. s31–s42, Feb. 2012.

[3] P. J. Winzer and G. J. Foschini, "MIMO capacities and outage probabilities in spatially multiplexed optical transport systems," *Opt. Exp.*, vol. 19, no. 17, pp. 16680–16696, Aug. 2011.

[4] R. Essiambre and R. W. Tkach, "Capacity trends and limits of optical communication networks," in *Proc. IEEE*, vol. 100, no. 5, pp. 1035–1055, May 2012.

[5] R. E. Freund, C.-A. Bunge, N. N. Ledentsov, D. Molin, and C. Casper, "High speed transmission in multi-mode fibers," presented at the *Opt. Fiber Commun. Conf.*, San Diego, CA, USA, Mar. 2009, Paper OMS1.

[6] E. Ip, A. P. T. Lau, D. J. F. Barros, and J. M. Kahn, "Coherent detection in optical fiber systems," *Opt. Exp.*, vol. 16, no. 2, pp. 753–791, Jan. 2008.

[7] E. Ip and J. M. Kahn, "Fiber impairment compensation using coherent detection and digital signal processing," *J. Lightw. Technol.*, vol. 28, no. 4, pp. 502–519, Feb. 2010.

[8] P. J. Winzer, "Energy-efficient optical transport capacity scaling through spatial multiplexing," *IEEE Photon. Technol. Lett.*, vol. 23, no. 13, pp. 851–853, Jul. 2011.

[9] M. B. Shemirani, W. Mao, R. A. Panicker, and J. M. Kahn, "Principal modes in graded-index multimode fiber in presence of spatial and polarization-mode coupling," *J. Lightw. Technol.*, vol. 27, no. 10, pp. 1248–1261, May 15, 2009.

[10] K.-P. Ho and J. M. Kahn, "Statistics of group delays in multimode fiber with strong mode coupling," *J. Lightw. Technol.*, vol. 29, no. 21, pp. 3119–3128, Nov. 2011.

[11] C. D. Poole and J. Nagel, "Polarization effects in lightwave systems," in *Optical Fiber Telecommunications*, vol. III-A, I. P. Kaminow and T. L. Koch, Eds. San Diego, CA, USA: Academic, 1997, pp. 114–161.

[12] F. Corsi, A. Galtarossa, and L. Palmieri, "Analytical treatment of polarization dispersion in single-mode fibers by means of backscattering signal," *J. Opt. Soc. Amer. A*, vol. 16, pp. 574–583, 1999.

[13] D. Marcuse, *Theory Dielectric Optical Waveguides*, 2nd ed. New York, NY, USA: Academic, 1991.

[14] K.-P. Ho and J. M. Kahn, "Mode-dependent loss and gain: Statistics and effect on mode-division multiplexing," *Opt. Exp.*, vol. 19, no. 17, pp. 16612–16635, Aug. 2011.

[15] K.-P. Ho and J. M. Kahn, "Frequency diversity in mode-division multiplexing systems," *J. Lightw. Technol.*, vol. 29, no. 24, pp. 3719–3726, Dec. 2011.

[16] G. D. Marshall et al. *et al.*, "Point-by-point written fiber-Bragg gratings and their application in complex grating designs," *Opt. Exp.*, vol. 18, no. 19, pp. 19844–19859, 2010.

[17] S. Ö. Arik, D. Askarov, and J. M. Kahn, "Adaptive frequency-domain equalization in mode-division multiplexing systems," *J. Lightw. Technol.*, vol. 32, no. 10, pp. 1841–1852, May 15, 2014.

[18] Y. Lu, W. Huang, and S. Jian, "Full vector complex coupled mode theory for tilted fiber gratings," *Opt. Exp.*, vol. 18, pp. 713–725, 2010.

[19] D. B. Stegall and T. Erdogan, "Leaky cladding mode propagation in long-period fiber grating devices," *IEEE Photon. Technol. Lett.*, vol. 11, no. 3, pp. 343–345, Mar. 1999.

[20] Y.-C. Lu, L. Yang, W.-P. Huang, and S.-S. Jian, "Unified approach for coupling to cladding and radiation modes in fiber Bragg and long-period gratings," *J. Lightw. Technol.*, vol. 27, no. 11, pp. 1461–1468, Apr. 2009.
[21] A. M. Vengsarkar, P. J. Lemaire, J. B. Judkins, V. Bhatia, T. Erdogan, and J. E. Sipe, "Long period gratings as band-rejection filters," *J. Lightw. Technol.*, vol. 14, no. 1, pp. 58–65, Jan. 1996.
[22] Y. Lu, L. Yang, W. Huang, and S. Jian, "Improved full-vector finite-difference complex mode solver for optical waveguides of circular symmetry," *J. Lightw. Technol.*, vol. 26, no. 13, pp. 1868–1876, Jul. 1, 2008.
[23] D. Marcuse, "Losses and impulse response of a parabolic index fiber with random bends," *Bell Syst. Tech. J.*, vol. 52, no. 8, pp. 1423–1437, Oct. 1973.
[24] S. Fan and J. M. Kahn, "Principal modes in multi-mode waveguides," *Opt. Lett.*, vol. 30, no. 2, pp. 135–137, Jan. 2005.
[25] S. Leon-Saval, N. Fontaine, J. Salazar-Gil, B. Ercan, R. Ryf, and J. Bland-Hawthorn, "Mode-selective photonic lanterns for space-division multiplexing," *Opt. Exp.*, vol. 22, pp. 1036–1044 2014.
[26] M. Tokuda, S. Seikai, K. Yoshida, and N. Uchida, "Measurement of baseband frequency response of multimode fibre by using a new type of mode scrambler," *Electron. Lett.*, vol. 13, no. 5, pp. 146–147, 1977.
[27] M. Ikeda, Y. Murakami, and K. Kitayama, "Mode scrambler for optical fiber," *Appl. Opt.*, vol. 16, no. 4, pp. 1045–1049, 1977.
[28] L. Su, K. S. Chiang, and C. Lu, "Microbend-induced mode coupling in a graded-index multimode fiber," *Appl. Opt.*, vol. 44, no. 34, pp. 7394–7402, 2005.
[29] W.F. Love, "Novel mode scrambler for use in optical-fiber bandwidth measurements," presented at the *Opt. Fiber Commun. Conf.*, Washington, DC, USA, 1979, Paper ThG2.
[30] Y. Koyamada, T. Horiguchi, M. Tokuda, and N. Uchida, "Theoretical analysis of optical fiber mode exciters constructed with alternate concatenation of step-index and graded-index fibers," *Electron. Commun. Jpn.*, vol. 68, pp. 66–74, 1985.

Authors' biographies not available at the time of publication.